

Vibrational spectra and crystal structure of $(XeF_5)_2NiF_6$ and its decomposition in the laser beam followed by raman spectroscopy

A. JESIH, K. LUTAR, I. LEBAN and B. ŽEMVA
“Jožef Stefan” Institute, 61111 Ljubljana, Slovenia, Yugoslavia

(Received November 27, 1990, accepted January 22, 1991.)

ABSTRACT. - Vibrational spectra of $(XeF_5)_2NiF_6$ show that it is XeF_5^+ salt. $(XeF_5)_2NiF_6$ decomposes in the laser beam at 79 K to xenon tetrafluoride, fluorine and nickel fluoride what is the unique case among known xenon(VI) fluorometalates. This phenomenon could possibly be explained by electron transfer through the common fluorine ligands bridging xenon and nickel. $(XeF_5)_2NiF_6$ crystallizes in the orthorhombic space group Pbca with $a = 18.837(2)$, $b = 11.148(2)$, $c = 10.952(1)$ Å, $V = 2299.9(5)$ Å³, $Z = 8$ and $d_{\text{cal}} = 3.610$ g/cm³. The structure was solved by Patterson method and refined to the final conventional R and R_w values of 0.056 and 0.069 for 1084 observed reflections ($I > 2.5 \sigma(I)$). The structure consists of XeF_5^+ and NiF_6^{2-} entities. The anion is essentially octahedral, with an average Ni-F bond distance of 1.77(2) Å. The cations are close to the C_{4v} symmetry with an average Xe-F^{ax} distance of 1.82(1) Å, an average Xe-F^{eq} distance of 1.84(1) Å, and an average F^{ax}-Xe-F^{eq} angle of 78.9(9)°. One cation acts as a bridging group to two NiF_6^{2-} anions, whereas the second cation is linked only to one anion thus forming closed dimeric rings what represents the unique structure of this type.

INTRODUCTION

In an attempt to produce xenon(VI) fluoronickelates(IV) a similar synthetic route to that employed in making $XeF_5^+AgF_4^-$ [1] was used. Nickel difluoride was treated with krypton difluoride (an extraordinary powerful oxidizer [2]) in anhydrous hydrogen fluoride (AHF) and in

the presence of fluorobase, xenon hexafluoride. Two new xenon(VI) fluoronickelates(IV) were obtained: $4\text{XeF}_6 \cdot \text{NiF}_4$ [3] and $2\text{XeF}_6 \cdot \text{NiF}_4$. The first one is thermally unstable and it decomposes into the 2:1 compound and xenon hexafluoride in a dynamic vacuum already at room temperature. The 2:1 compound is stable in a dynamic vacuum at room temperature but it decomposes in the laser beam even at 77 K giving xenon tetrafluoride. Further the X-ray powder photographs show that $2\text{XeF}_6 \cdot \text{NiF}_4$ is not similar to $2\text{XeF}_6 \cdot \text{PdF}_4$ [4]. As the decomposition of xenon(VI) fluorometalates to xenon tetrafluoride was not noticed up to now, it was decided to elucidate this problem. This paper describes vibrational spectra and crystal structure of the 2:1 compound and its decomposition in the laser beam followed by Raman spectroscopy.

EXPERIMENTAL

Apparatus and Reagents used in this work are described elsewhere [3].

Instrumentation. Raman spectra were recorded using a Spex 1401 double monochromator instrument and Spex triplemate spectrometer with multi-channel optical analyser (Spectroscopy Instruments). As exciting radiation, the 514.5 nm line of an Ar^+ laser and 674.1 nm line of a Kr^+ laser (Coherent Radiation) were used. Powdered samples were loaded into quartz capillaries in a dry box and temporarily plugged with Kel-F grease. They were sealed with a small flame outside the dry box. Spectra were recorded at 77 K by placing the sample tube inside a partly unsilvered glass Dewar filled with liquid nitrogen. Some spectra were recorded also in the rotating cell made of Teflon and with a sapphire window. Infrared spectra were recorded using Fourier transform spectrometer (Perkin Elmer 7100). Spectra were obtained by dusting samples onto silver chloride plates which were later sandwiched in a leak tight brass holder. Other instrumentation (X-ray powder diffraction method and magnetic susceptibility) are described elsewhere [3].

Preparation of $(\text{XeF}_5^+)_2\text{NiF}_6^{2-}$ Single Crystals. Since the solubility of $(\text{XeF}_5^+)_2\text{NiF}_6^{2-}$ in AHF is moderate, crystals were grown by recrystallizing $(\text{XeF}_5^+)_2\text{NiF}_6^{2-}$ in AHF. To prevent solvolysis some xenon hexa-

fluoride and krypton difluoride were added to AHF which was before thoroughly pretreated with K_2NiF_6 and finally with KrF_2 . After some weeks AHF was pumped off at room temperature. The remaining red crystals were loaded in 0.5 quartz cappilaries in a dry box. The capillaries were carefully pretreated before use (heated for 24 hours at 400°C and exposed to elemental fluorine).

Structural Determination of $(\text{XeF}_5^+)_2\text{NiF}_6^{2-}$. The crystals were of poor quality, very sensitive to traces of moisture. Several crystals were mounted in quartz capillaries and tested on CAD-4 automated diffractometer. Details of procedures used for data collection and structure determination are given in Table I. Atomic coordinates and temperature factors are given in Table II and selected bond lengths and angles in Table III.

TABLE I. Crystal data and details of structure determination and refinement for $(\text{XeF}_5)_2\text{NiF}_6$

formula	$(\text{XeF}_5)_2\text{NiF}_6$	temp, K	293(1)
mol wt	625.3	scan technique	$\omega-2 \theta$
space group ^a	Pbca	2 θ scan width, deg	0.8+0.3 tan θ
cryst. system	orthorhombic	scan rate, deg/min	5.49-16.48
a, Å	18.837(2)	bkgd	0.25 of scan time at each of scan limits
b, Å	11.148(2)	2 θ _{max} , deg	60
c, Å	10.952(1)	max scan time, s	10
vol, Å ³	2299.9(5)	reference reflcns	3 after each hour
z	8	orient reflcns	3 after 500 reflcns
d _{calcd} , g cm ⁻³	3.610	intensity decrease, %	16
shape of cryst	irregular	measured reflcns	5786
colour	dark red	averaged reflcns	2784
F(000)	2240	mean discr on I, %	2.9
diffractometer	CAD-4 Enraf Nonius		
data collected	+h, ±k, +l		
radiation	MoK α		
monochromator,	graphite (12.1)		
(angle, deg)			

TABLE I (cont.)

observed reflcns ^c	1084	R, R_w^h	0.056, 0.069
criterion	$1 > 2.5 \sigma (I)$	weight	$0.82(\frac{\sigma}{F_0})^2_{-1} + 0.0026(\frac{\sigma}{F_0})^2_0$
$\mu, \text{ cm}^{-1}$	76.8	no. of params	172
absor corr ^d	empirical	ratio of observns to params	6.30
program used	SHELX 76 ^e , GX ^f	max shift/error	0.072
scattering factors	neutral atoms ^g	residual electr density, $e/\text{\AA}^3$	-1.21 to +1.48

^aInternational Tables for X-ray Crystallography; Kynoch: Birmingham, England, 1965; Vol. I. ^bCell dimensions were determined by least-squares fit of the setting angles of 25 reflections with θ in the range 7-9°. ^cDue to large discrepancies reflections 0 2 2, 2 0 2, 24 4 3, 22 2 7 and 14 3 12 were removed from the data set. Ugozzoli, F.: Comput. Chem., 11, 1987, 109-120. ^dSheldrick, G.: SHELX76 System of Computing Programs; University of Cambridge: Cambridge, England, 1976. Gilmore, C.J., Mallinson, P.R. and Muir, K.W. The GX Package; University of Glasgow; Glasgow, Scotland, 1985.

^gInternational Tables for X-ray Crystallography; Kynoch: Birmingham, England, 1974; Vol. IV. The quantity minimized in the least-squares procedures is

$$w(|F_o| - |F_c|)^2. R = \sqrt{\sum |F_o| - |F_c| / \sum |F_o|};$$

$$R_w = [\sum w(|F_o| - |F_c|)^2 / \sum w(F_o)]^{1/2}.$$

TABLE II. Fractional atomic coordinates and isotropic temperature factors (\AA^2), with estimated standard deviations in parentheses. For anisotropic atoms, the equivalent isotropic temperature factors are shown.

	X/A	Y/B	Z/C	U
Xe1	0.49182(10)	0.19221(10)	0.19374(10)	0.039
Xe2	0.78923(10)	-0.00384(20)	-0.01788(10)	0.049
Ni	0.6224(2)	0.0374(3)	0.0240(3)	0.042
F1	0.4709(7)	0.2997(14)	0.3125(13)	0.075
F2	0.4848(8)	0.0902(16)	0.3260(13)	0.081
F3	0.5813(8)	0.2360(14)	0.2426(14)	0.080
F4	0.4872(9)	0.3302(13)	0.1036(17)	0.097
F5	0.3938(7)	0.1966(18)	0.1908(15)	0.102
F6	0.8831(7)	-0.0360(17)	-0.0400(17)	0.107
F7	0.8090(9)	-0.0934(19)	0.1179(19)	0.121
F8	0.8324(10)	0.1253(19)	0.0575(21)	0.133
F9	0.8070(9)	0.0733(20)	-0.1629(16)	0.115
F10	0.7832(9)	-0.1395(17)	-0.1079(20)	0.119
F11	0.5771(7)	0.0184(11)	0.1619(12)	0.053
F12	0.6743(7)	-0.0952(10)	0.0469(16)	0.064
F13	0.6932(6)	0.1132(12)	0.0991(14)	0.058
F14	0.5564(7)	-0.0421(16)	-0.0548(15)	0.101
F15	0.5746(7)	0.1729(13)	0.0072(12)	0.065
F16	0.6725(7)	0.0599(14)	-0.1134(12)	0.066

TABLE III. Selected bond lengths and angles for $(\text{XeF}_5^+)_2 \text{NiF}_6^{2-}$

Xe1 - F1	1.81(2)	Xe1 - F2	1.85(2)
Xe1 - F3	1.84(2)	Xe1 - F4	1.83(2)
Xe1 - F5	1.85(2)	Xe2 - F6	1.82(2)
Xe2 - F7	1.83(3)	Xe2 - F8	1.85(3)
Xe2 - F9	1.84(2)	Xe2 - F10	1.81(2)
Ni - F11	1.75(2)	Ni - F12	1.79(2)
Ni - F13	1.78(2)	Ni - F14	1.75(2)
Ni - F15	1.77(2)	Ni - F16	1.79(2)
F1 - Xe1 - F2	80.1(8)	F1 - Xe1 - F3	79.3(7)
F1 - Xe1 - F4	79.7(8)	F1 - Xe1 - F5	77.1(8)
F2 - Xe1 - F3	90.0(7)	F2 - Xe1 - F4	159.7(8)
F2 - Xe1 - F5	87.6(8)	F3 - Xe1 - F4	88.7(8)
F3 - Xe1 - F5	156.4(8)	F4 - Xe1 - F5	85.4(8)
F6 - Xe2 - F7	78.6(9)	F6 - Xe2 - F8	77.6(9)
F6 - Xe2 - F9	78.5(9)	F6 - Xe2 - F10	79.9(8)
F7 - Xe2 - F8	88.4(10)	F7 - Xe2 - F9	157.1(8)
F7 - Xe2 - F10	90.0(10)	F8 - Xe2 - F9	86.6(10)
F8 - Xe2 - F10	157.3(9)	F9 - Xe2 - F10	86.1(10)
F11 - Ni - F12	92.7(7)	F11 - Ni - F13	91.4(7)
F11 - Ni - F14	91.0(7)	F11 - Ni - F15	86.8(7)
F11 - Ni - F16	177.3(7)	F12 - Ni - F13	85.3(7)
F12 - Ni - F14	92.2(8)	F12 - Ni - F15	176.6(7)
F12 - Ni - F16	86.9(8)	F13 - Ni - F14	176.7(7)
F13 - Ni - F15	91.4(7)	F13 - Ni - F16	85.9(7)
F14 - Ni - F15	91.1(8)	F14 - Ni - F16	91.7(7)
F15 - Ni - F16	93.5(7)		

Additional interatomic distances

Xe1 - F11 _i	2.54(1)
Xe1 - F14 _i	2.44(2)
Xe1 - F15	2.58(1)
Xe2 - F12	2.50(1)
Xe2 - F13	2.57(1)
Xe2 - F16	2.54(1)

Additional angles

F(1)-Xe(1)-F(11) _i	137.8(5)
F(1)-Xe(1)-F(14) _i	145.2(5)
F(1)-Xe(1)-F(15)	139.0(6)
F(6)-Xe(2)-F(12)	143.1(7)
F(6)-Xe(2)-F(13)	148.1(7)
F(6)-Xe(2)-F(16)	147.4(7)

Estimated standard deviations in parentheses

Symmetry code: i) 1-x, -y, -z

Description of the $(\text{XeF}_5^+)_2\text{NiF}_6^{2-}$ Structure. The structural unit contains two crystallographically distinct XeF_5 groups and an NiF_6 group (Fig. 1 and 2). The NiF_6 group is almost octahedral. As may be determined from Table III, the average Ni-F distance is $1.77(2)$ Å. All cis F-Ni-F angles are within 5° of 90° . The two XeF_5 groups are similar, each being approximately C_{4v} symmetry species, with an average $\text{F}_{\text{ax}}\text{-Xe-F}_{\text{eq}}$ angle of $\sim 79^\circ$. The average Xe-F_{ax} interatomic distance of the two crystallographically distinct species is $1.82(1)$ Å and the axial Xe-F distance for each species does not depart significantly from this mean value. The average value for all Xe-F_{eq} interatomic distances is $1.84(1)$ Å. Only one Xe-F_{eq} distance [$\text{Xe}(2)\text{-F}(10) - 1.81$ Å] significantly departs from this mean value.

Each Xe atom of each XeF_5 group makes three contacts with NiF_6 groups. $\text{Xe}(1)$ makes one short contact with one NiF_6 group $\text{Xe}(1)\text{-F}(14)^i$ and two somewhat longer contacts to a second NiF_6 group, while $\text{Xe}(2)$ makes three contacts with only one NiF_6 group. These Xe...F contacts link XeF_5 and NiF_6 groups into "rings" containing two moieties.

It should be noted that the three F ligands of the NiF_6 groups which make close approach to Xe atom, make this symmetrically with respect to the pseudo-fourfold axis of each XeF_5 group. Thus the corresponding $\text{F}_{\text{ax}}\text{-Xe...F}$ angles all lie within the range $138\text{-}148^\circ$. The center of inversion is in the hole between two NiF_6 groups and two XeF_5 groups with $\text{Xe}(1)$.

RESULTS AND DISCUSSION

Vibrational Analysis

The vibrational spectra of $(\text{XeF}_5^+)_2\text{NiF}_6^{2-}$ are given in Table IV. The XeF_5^+ cation with approximately C_{4v} symmetry has the vibrational representation: $3a_1 + 2b_1 + b_2 + 3e$. All modes are Raman active but only $3a_1 + 3e$ are infrared active. The observed lines were assigned on the basis of their relative intensities and by comparison with the spectra of related molecules [5,6].

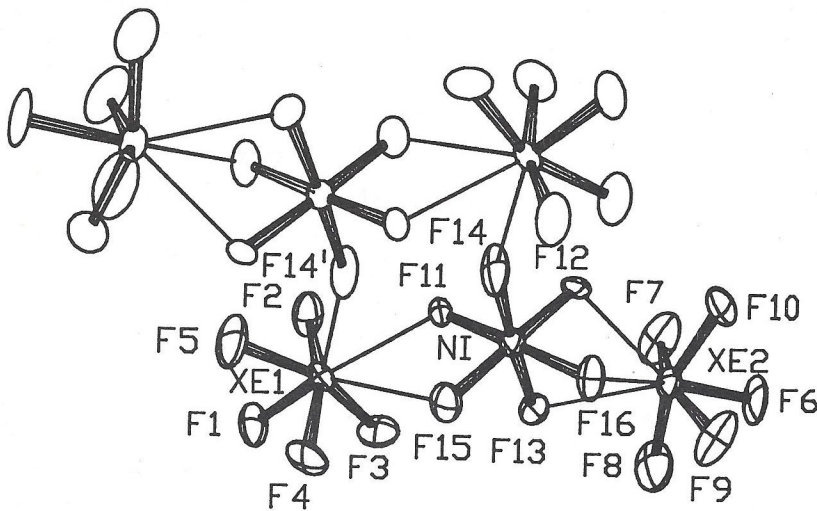


Fig. 1. Ortep diagram of dimeric ring in $(\text{XeF}_5)_2 \text{NiF}_6$

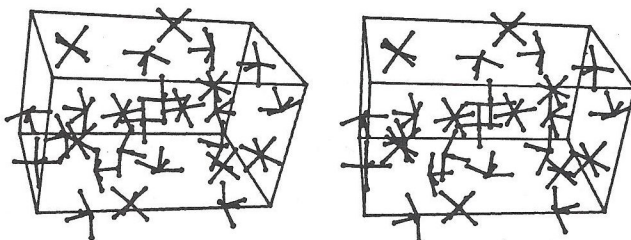


Fig. 2. Stereogram of the $(\text{XeF}_5)_2 \text{NiF}_6$ unit cell

The strong lines at ca 650 cm^{-1} and 582 cm^{-1} are ν_1 and ν_2 , the a_1 stretching fundamentals. ν_7 (e), the degenerate stretching mode of the basal XeF_4 unit, should generate a strong infrared absorption, and it is assigned at 636 cm^{-1} and 657 cm^{-1} , since the infrared spectrum of $(\text{XeF}_5^+)_2 \text{NiF}_6^{2-}$ has its strongest absorption at these frequencies. The assignment of the two b_1 fundamentals ν_4 and ν_5 is based on their infrared inactivity and relative weakness of their

TABLE IV. Raman and infrared frequencies (cm^{-1}) and assignment
for $(\text{XeF}_5^+)_2\text{NiF}_6^{2-}$

IR a)	$(\text{XeF}_5^+)_2\text{NiF}_6^{2-}$ Raman b)		Assignment
		XeF_5^+	NiF_6^{2-}
660 sh	657 (94) 650 (100)	$\nu_7(\text{e})$ $\nu_1(\text{a}_1)$	ν_3
636 vs	636 (66) 620 (7) 600 (15)	$\nu_7(\text{e})$ $\nu_4(\text{b}_1)$	
583 m	582 (55) 570 (28) 520 (2)	$\nu_2(\text{a}_1)$	ν_1 ν_2
430 m	404 (5)	$\nu_8(\text{e})$	
388 m	371 (7)	$\nu_3(\text{a}_1)$	
363 m	303 (6) 292 (6)	$\nu_6(\text{e})$	ν_4 ν_5
	236 (6) 216 (4) 196 (4)	$\nu_5(\text{b}_1)$ $\nu_9(\text{e})$	

a) sh-shoulder, vs-very strong, m-medium

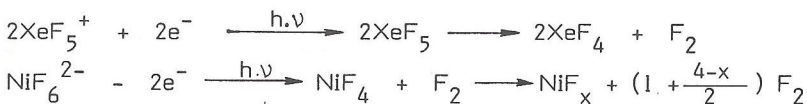
b) Spectrum was obtained using Spex 1401 double monochromator.

Relative intensities are in parentheses.

Raman lines. The Raman line at 371 cm^{-1} is $\nu_3(\text{a}_1)$. The splitting of the line ca 400 cm^{-1} in several XeF_5^+ salts and its high intensity in infrared spectrum suggest, that it is indeed $\nu_8(\text{e})$. The lines at 303 cm^{-1} and 292 cm^{-1} and at 216 cm^{-1} and 196 cm^{-1} are assigned to $\nu_6(\text{e})$ and $\nu_9(\text{e})$ respectively.

The other Raman and infrared lines could be attributed to the NiF_6^{2-} anion on the basis of comparison with Raman and infrared spectra of K_2NiF_6 [7] and $(\text{NH}_4)_2\text{NiF}_6$ [8]. The bands at 570 cm^{-1} and 520 cm^{-1} can be therefore assigned to ν_1 and ν_2 respectively, whereas ν_5 and ν_3 components are present in the band at 303 cm^{-1} in Raman spectrum and at 660 cm^{-1} in infrared spectrum.

During the recording of the Raman spectra of $(\text{XeF}_5)_2 \text{NiF}_6$, the ν_1 and ν_4 modes of xenon tetrafluoride were also noticed among the other lines. The intensity of both lines was increasing with the exposure time to the laser beam (Fig. 3). XeF_4 was present regardless of the wave length of the laser beam or the techniques used for recording spectra (rotating cell, recording spectra at 77 K). This is the first example of such decomposition of XeF_5 salt. This phenomenon could possibly be explained by electron transfer through the common fluorine ligands which bridge nickel and xenon. Overall reaction mechanism could be written as follows:



$$3 > x > 2$$

The final decomposition products are xenon tetrafluoride, elemental fluorine and nickel fluoride in which mole ratio $\text{F} : \text{Ni}$ is between two and three thus showing that some higher nickel fluorides are still present. Although the Raman lines of nickel fluoride are weak, it was shown by separate experiment that under the conditions used for recording the spectra the lines of elemental fluorine and nickel fluoride could not be detected. Further it was noticed that the spectrum does not change with the time, except ν_1 and ν_4 modes of XeF_4 thus showing that $(\text{XeF}_5^+)(\text{NiF}_5^-)$ is not present as an intermediate product. The obtained spectrum could therefore be attributed only to $(\text{XeF}_5)_2 \text{NiF}_6$.

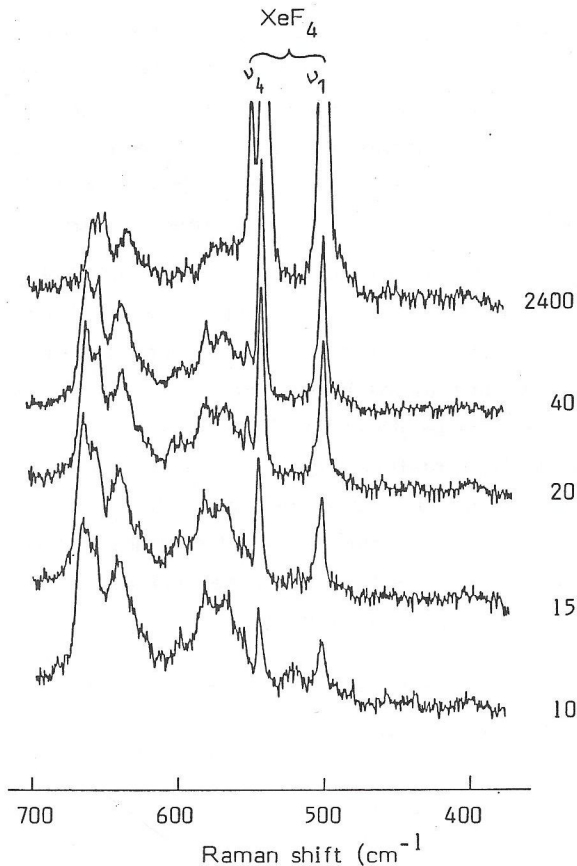


Fig. 3. Decomposition of $(\text{XeF}_5)_2\text{NiF}_6$ in the laser beam as a function of time. The number at the right end of the curve represents the exposure time of the sample (in seconds) to the laser beam. The spectra were obtained using Spex triplemate spectrometer with multi-channel optical analyser.

Discussion of the Structure

The crystal structure of $2\text{XeF}_6\cdot(\text{XeF}_5)_2\text{NiF}_6$ confirms earlier speculations [4] that all complexes of the type $2\text{XeF}_6\cdot\text{MF}_4$ (M = four valent metal) are XeF_5^+ salts. A low spin t_{2g}^6 Ni(IV) electron configuration is expected to be akin to the configurations of

Pt(IV) and Pd(IV) and like them to favor a regular octahedral MF_6^{2-} species. Like in $(\text{XeF}_{11}^+)_2 \text{NiF}_6^{2-}$ [3], also in this case NiF_6^{2-} is not perfectly octahedral but slightly distorted as a consequence of interactions with XeF_5^+ cations. The average Ni-F distance of 1.77(2) Å agrees well with the average Ni-F distance in other Ni(IV) complexes: 1.78(1) Å in $(\text{XeF}_{11}^+)_2 \text{NiF}_6^{2-}$ [3], 1.78 Å in M_2NiF_6 ($\text{M} = \text{Rb}, \text{K}$) [9] and 1.776(8) Å in K_2NiF_6 [10].

The structure of $(\text{XeF}_5^+)_2 \text{NiF}_6^{2-}$ is of most interest for the cation-anion interactions. Both XeF_5^+ groups are similar to cation groups previously found in other XeF_5^+ salts [4]. The average $\text{Xe}-\text{F}_{\text{ax}}$ distance is 1.82 Å and is shorter than the average $\text{Xe}-\text{F}_{\text{eq}}$ bond length which is 1.84(1) Å. Like in $(\text{XeF}_5^+)_2 \text{PdF}_6$ [4] each XeF_5^+ species of $(\text{XeF}_5^+)_2 \text{NiF}_6^{2-}$ is coordinated to three F ligands which lie approximately on a conical surface, the axis of which is coincident with the symmetry axis of the XeF_5^+ . If we describe XeF_5^+ as a pseudo-octahedral species in which the nonbonding valence electron pair occupies the Xe coordination site trans to the axial bond, the position of the F ligands is between this electron pair and equatorial fluorines. The main difference between $(\text{XeF}_5^+)_2 \text{PdF}_6^{2-}$ and $(\text{XeF}_5^+)_2 \text{NiF}_6^{2-}$ is that in the case of palladium each xenon atom is coordinated to two PdF_6^{2-} groups thus forming rings which are further linked to adjoining rings by Pd-F-Xe bonds while in the case of nickel we have finite rings: one XeF_5^+ (Xe-2) is coordinated only to one NiF_6^{2-} , while one XeF_5^+ (Xe-1) is coordinated to two NiF_6^{2-} groups, thus forming isolated dimeric rings.

ACKNOWLEDGEMENTS

The authors are grateful to Dr. M. Zgonik for recording Raman spectra on Spex Triplemate Spectrometer and to the Secretariat for Research and Technology of Slovenia for the financial support.

REFERENCES

- [1] K. LUTAR, A. JESIH and B. ŽEMVA, *Rev. Chim. Min.*, 1986, 23, p. 565.
- [2] N. BARTLETT and F.O. SLADKY, *The Chemistry of Krypton, Xenon and Radon*, in *Comprehensive Inorganic Chemistry*, Vol. I. (Ed. J.C. Bailar and A.F. Trotman-Dickenson) Pergamon: Oxford and New York, 1973, p. 245.
- [3] A. JESIH, K. LUTAR, I. LEBAN and B. ŽEMVA, *Inorg. Chem.*, 1989, 28, p. 2911.
- [4] K. LEARY, D.H. TEMPLETON, A. ZALKIN and N. BARTLETT, *Inorg. Chem.*, 1973, 12, p. 1726.
- [5] C.J. ADAMS and N. BARTLETT, *Isr. J. Chem.*, 1978, 17, p. 114.
- [6] K.O. CHRISTE, E.C. CURTIS and R.D. WILSON, *Inorg. Nucl. Chem., Suppl.*, 1976, p. 159.
- [7] M.J. REISFELD, *J. Molec. Spec.*, 1969, 29, p. 120.
- [8] K.O. CHRISTE, *Inorg. Chem.*, 1977, 16, p. 2238.
- [9] R. HOPPE and T. FLEISCHER, *J. Fluorine Chem.*, 1978, 11, p. 251.
- [10] J.C. TAYLOR and P.W. WILSON, *J. Inorg. Nucl. Chem.*, 1974, 36, p. 1561.